

# Preliminary study of human breast tissue using synchrotron radiation combining WAXS and SAXS techniques

A.L.C. Conceição<sup>1</sup>, M. Antoniassi<sup>1</sup>, M.E. Poletti<sup>1</sup>, L.V. Caldas<sup>2</sup>

<sup>1</sup> Departamento de Física e Matemática, Faculdade de Filosofia, Ciências e Letras de Ribeirão Preto, Universidade de São Paulo, Ribeirão Preto, SP, Brazil. poletti@ffclrp.usp.br

<sup>2</sup> Instituto de Pesquisas Energéticas e Nucleares, Comissão Nacional de Energia Nuclear, São Paulo, SP, Brazil

## Abstract

Using synchrotron radiation, we combined simultaneously wide angle x-ray scattering (WAXS) and small angle x-ray scattering (SAXS) techniques to obtain the scattering profiles of normal and neoplastic breast tissues samples at the momentum transfer range  $6.28\text{nm}^{-1} \leq Q (=4\pi \cdot \sin(\theta/2)/\lambda) \leq 50.26\text{nm}^{-1}$  and  $0.15\text{nm}^{-1} \leq Q \leq 1.90\text{nm}^{-1}$ , respectively. The results obtained show considerable differences between the scattering profiles of these tissues. We verified that the combination of some parameters (ratio between glandular and adipose peak intensity and third-order axial peak intensity) extracted from scattering profiles can be used for identifying breast cancer.

*Keywords:* x-ray scattering; scattering profiles; mammography; breast cancer

## 1. Introduction

Breast cancer is the most frequently incident in women and accounts for almost 20% of all cancer deaths (Rogers et al., 1999). Mammography is the principal technique for early detection of breast cancer, but it is neither 100% sensitive nor 100% specific, presenting both false negative and false positive diagnoses and leading to undiagnosed cancer and inappropriate biopsies. This fact is mainly due to small differences in attenuation properties of the breast tissues (Kidane et al., 1999, Tomal et al. 2008) and the non ideal observer performance. Several complementary techniques have been introduced in order to eliminate these sources of mistakes, as for example sonography and magnetic resonance imaging (MRI) correlations, tomosynthesis, phase-contrast imaging. On the other hand, recent investigations have shown that x-ray scattering analysis could be used for early detection and diagnosis of breast cancer (Kidane et al., 1999; Speller et al., 1999; Lewis et al. 2000; Poletti et al., 2002a; Fernández et al. 2005; Round et al. 2005; Cunha et al. 2006; Griffiths et al., 2007 and Oliveira et al., 2008). The motivation of these works

is the important fact that the photons that have been scattered inside the breast had a close contact with the atomic structure of the tissues; carrying this information with them (Speller et al., 1999). Consequently, if cancer cells cause changes into the biological structures of tissues that they attack, this alteration will be present in the scattering profile (the distribution of the number of scattering photons as function of scattering angle or momentum transfer) of the tissue, being this distribution due to the collective scattering effects due to atom, molecule and supra-molecular arrangements in the material. For a given energy, the scattering effects in high angles are due to the internal atomic structure of the material, therefore, the interferences among the several atoms that compose the tissue are not detected (Poletti et al., 2002b). In intermediate or wide angles, atomic or molecular interferences appear in the scattering profile, while in small angles this profile shows information about supramolecular structures present in tissues (Fernández et al., 2005). These effects of interferences cause a unique and characteristic scattering profile for each material (or tissue), which can be computed if the structural parameters are known (spatial distribution of charge, distance among atoms and so on). As these parameters are, in general, unknown a priori, the scattering profile should be experimentally measured.

Usually two techniques are used to measure scattering profiles from human breast tissues: WAXS (wide angle x-ray scattering) and SAXS (small angle x-ray scattering). WAXS technique allows obtaining a spatial distribution of smallest cell structures that compose the tissues, as for example water and fatty acid (Evans et al. 1991; Tartari et al., 1997; Kidane et al., 1999; Poletti et al., 2002a,c; Cunha et al. 2006; Griffiths et al., 2007; Oliveira et al. 2008). These works have shown that some parameters extracted from the scattering profile, as peak position, height and FWHM (Kidane et al., 1999), ratio of peaks intensities at 19.6 and 13.8 nm<sup>-1</sup> (Griffiths et al., 2007) and the complete shape (Cunha et al. 2006, Oliveira et al. 2008), could be used to differentiate between healthy and neoplastic human breast tissue. On the other hand, SAXS technique allows determining supramolecular system features, for example the protein collagen, the major structural component of the extra-cellular matrix in breast tissues (Rogers et al., 1999; Lewis et al 2000; Fernández et al 2004). Lewis et al. (2000) extracted two parameters (intensity of third-order peak and third-order axial spacing) from the scattering profiles and showed that the obtained values of these parameters are significantly different among normal tissue, benign and malignant diseases. Fernández et al. (2002, 2004) used the scattering profile to determine some characteristic parameters (as axial period, average x-ray scattering intensity, fibril diameter and packing) and concluded the each type of tissues can be classified by them. Round et al. (2005) used the complete curve of scattering intensity with respect to the

momentum transfer and reduced it using Principal Component Analysis (PCA) in order to classify normal and diseased tissues. Falzon et al. (2006) applied wavelet decomposition to SAXS image and showed that successful identification of breast tissues malignancy can be achieved using wavelet coefficients and supervised classification.

In summary, WAXS and SAXS experiments independently can provide important parameters to detect and diagnose a disease (cancer). Therefore it is expected that the combination of both techniques simultaneously can correlate structural changes at atomic level with changes at larger scales (Ali et al. 2004; Tartari et al., 2005). It also allows that several parameters be studied in a single experiments improving the diagnostic information present in the scattering profile. Therefore, in this preliminary study, both techniques were simultaneously used on each sample (normal and neoplastic breast tissue) to determinate the scattering profiles and to determine which parameters can be used to classify different human breast tissue. The authors are unaware of any work in the literature combining WAXS and SAXS techniques in a single experiment to try differentiate among healthy, benign and malignant human breast tissue.

## **2. Experimental Systems and Methods**

### *2.1. Breast Tissue Samples*

The breast tissue samples analyzed in this work were obtained from mastectomy and reduction mammoplasty procedures. After collected, they were histopathologically classified as normal tissues, fibroadenomas (benign disease) or carcinomas (malignant disease). Subsequently to collection and classification, the samples were stored within suitable receptacles and fixed in formalin (10% formaldehyde in water). A total of 8 samples were analyzed in this preliminary work, being: three normal tissues, three carcinomas and two fibroadenomas. At the moment of the measurements, the samples were cut to 10 mm x 2 mm x 1 mm, inserted into a sample-holder and covered at both sides by thin mica foils.

### *2.2. Experimental Set up*

The combination of WAXS with SAXS was implemented in D11A – SAXS at the synchrotron radiation source of the Laboratório Nacional de Luz Síncrotron (LNLS) in Campinas, Brazil. The experimental set up used in these experiments can be observed in figure 1. A focused monochromator of Si (111) was used in order to provide an x-ray beam of wavelength 1.48 Å and to reduce the irradiation area (1.0 mm x 0.5mm) on the sample. The detectors

for both techniques were two-dimension Fuji Bas III image plates. The WAXS image plate detector was fixed on a cylinder detector-holder focused on the sample and at a distance of 200mm to the sample, as shown in the figure 1, allowing a recording range of momentum transfer of  $6.28\text{nm}^{-1} < Q (=4\pi \cdot \sin(\theta/2)/\lambda) < 50.26\text{nm}^{-1}$ . The sample to SAXS image plate detector distance was fixed at 1.59 m and this space was evacuated using a vacuum chamber in order to minimize air scattering and absorption losses. A beam stop of 8 mm-diameter was inserted adjacent and centrally to detector in order to avoid the saturation of the detector produced by primary intensity. In this case the accessible momentum transfer ranges were  $0.15\text{nm}^{-1} < Q < 1.90\text{nm}^{-1}$ . Both image plates were read out and digitalized with a high resolution scanner (100  $\mu\text{m}$ ) MAR 300 of Molecular Dynamics®. The time of measurement was adjusted in order to assure statistical uncertainty smaller than 1% to the scattered photons intensity. Standard samples, alumina ( $\text{N}_2\text{O}_3$ ) and SilverBehenat ( $\text{CH}_3(\text{CH}_2)_{20}\text{COOAg}$ ), were used as a calibrant to WAXS and SAXS, respectively, in order to establish the correct reciprocal space scale of each pattern.

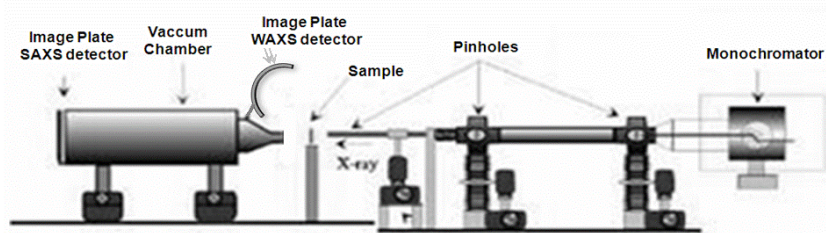


**Figure 1.** Experimental set up.

### 2.3. Data Reduction

All digitalized images (standards, samples and sample-holder) of WAXS and SAXS were processed using the software Fit2D, available by European Synchrotron Radiation Facility. From WAXS images, the distribution of scattered intensity as function of the momentum transfer was integrated at the vertical direction at the center of each strip, figure 2, while for SAXS images this integration was performed at both directions, meridian and equator, as is shown in figure 3 (Wilkinson et al., 2006). Several steps are necessary in order to obtain the linear differential scattering coefficient  $\mu_s$ , which is defined as  $\mu_s = n_v d\sigma/d\Omega$ , being  $n_v$  the number of molecules per unit of volume and  $d\sigma/d\Omega$  the total molecular differential cross-section. The first one is to correct the data for incident beam decay. Second, the number of photons originated from every other spurious scattering sources (sample-holder, collimators, etc) must be subtracted from the original data. Third, the resulting data have to be corrected for a

geometric self-attenuation factor. For WAXS experiment, this latter factor presents exponential behavior, and is obtained by Monte Carlo methods, while, for SAXS experiment this factor can be considered a constant value for each sample data, given that  $\cos(\theta) \approx 1$  (this factor corresponds to the transmission factor and it was measured at the moment of data collection). Finally, the last step consists in normalizing the data, by using a scaling factor, in order to obtain the absolute linear differential scattering cross section. The scaling factor is obtained from the ratio between theoretical, which can be obtained through IAM (Hubbel et al., 1975), and experimental values of  $\mu_s$  at higher momentum transfer, where interferences effects don't occur (Poletti et al., 2002b). Denoting  $I_{S+BG}(Q)$  and  $I_{BG}(Q)$  as the total (sample and background) and background scattering intensity, corrected for incident beam decay, respectively, the scattering profile ( $\mu_s$ ) can be determine using,

$$\mu_s(Q) = [I_{S+BG}(Q) \cdot A_{S+BG}(Q) - I_{BG}(Q) \cdot A_{BG}(Q)] \cdot C \quad (1)$$

where  $A(Q)$  correspond to geometric self-attenuation factor; the indexes **S** and **BG** into the brackets correspond to sample and background, respectively, and C is the scaling factor.

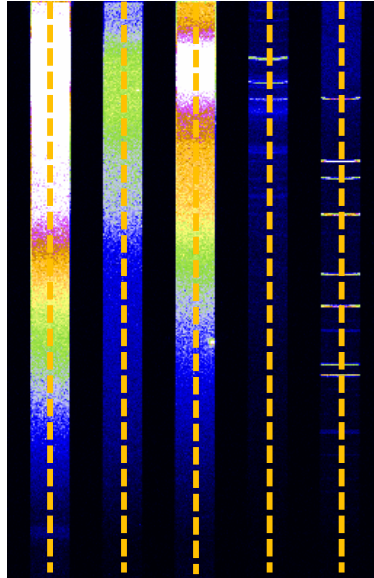


**Figure 2.** WAXS images. From left to right, each strip represents: three types of breast tissue, background signal and calibration sample.

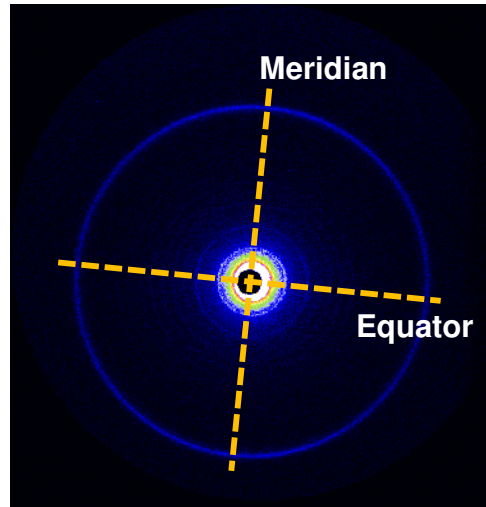


**Figure 3.** Example of SAXS experimental image with system of coordination marked.

### 3. Results and Discussion

Figures 4 and 5 show the mean scattering profiles for each group of tissues analyzed in this work for WAXS and SAXS, respectively. It should be note that the aim of this preliminary work was the identification of features that may be used to differentiate among normal, benign and malignant human breast tissue using WAXS and SAXS techniques simultaneously and not to perform a full molecular structure analysis of breast tissue.

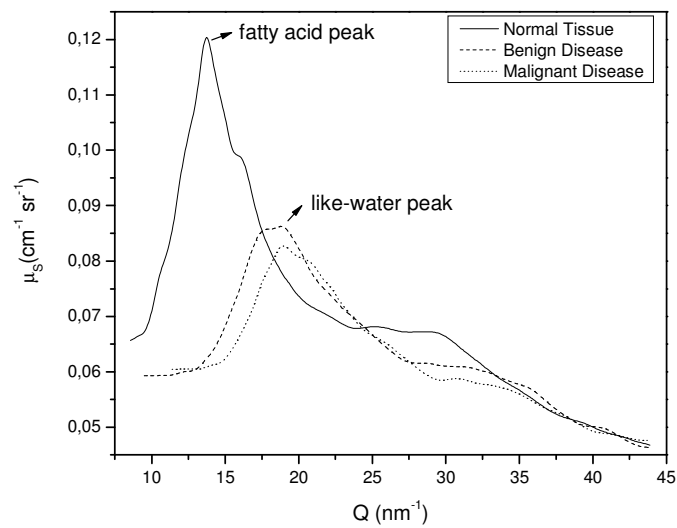


**Figure 4.** Mean WAXS profile of each type of breast tissue analyzed in this work.

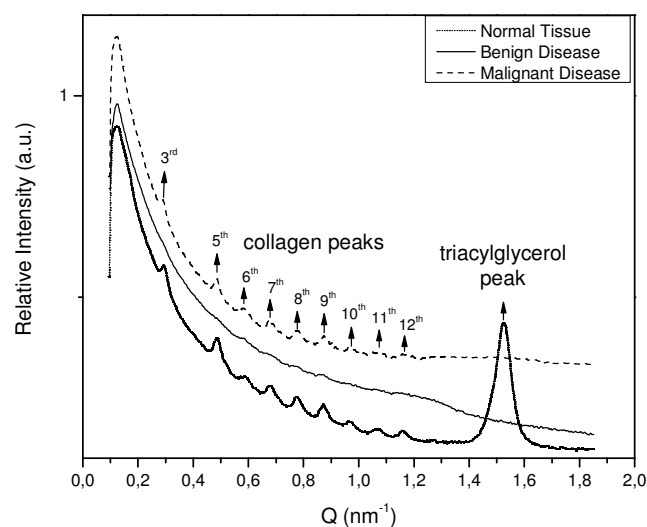


**Figure 5.** Mean SAXS profiles of each type of breast tissue analyzed.

Preliminary results based on the scattering profile obtained with WAXS technique show that all normal breast tissues have a first maximum peak at  $Q = 13.8 \text{ nm}^{-1}$  (Tartari et al., 1997; Peplow and Verghese, 1998; Kidane et al., 1999; Poletti et al., 2002a,c), which is related to structures of fatty acid, principal component of adipose cells (Tartari et al., 1997). For benign and malignant tissues, the maximum peak appear in another position ( $Q = 18.9 \text{ nm}^{-1}$ ), this peak position agreeing with previous works (Kidane et al., 1999; Griffiths et al., 2007; Oliveira et al. 2008) and being related probably to the high water-content in their constitution (Poletti et al., 2002a and Ryan et al., 2007). The only difference between benign and malignant tissues is the intensities of the peaks.

From SAXS scattering profiles, several peaks may be clearly seen in all samples studied, from 3<sup>rd</sup> ( $Q = 0.29 \text{ nm}^{-1}$ ) to 12<sup>th</sup> ( $Q = 1.17 \text{ nm}^{-1}$ ), corresponding to structures with a fundamental spacing of approximately 65 nm. This d-spacing is consequence of the staggered arrangement of tropocollagen within the fibrils (Bigi and Roveri, 1991, Lewis et al. 2000). Analyzing the scattering profiles shown in the Fig. 5, it was observed that the intensity of third order axial peak was greater in malignant tissues than in other ones. This observation is in agreement with Pucci-Minafra et al. (1993), who pointed that this is related with an increase of the specific surface area of new fibril collagen induced by cancerous cells. Additionally in the normal tissues, another peak arises at

$Q=1.51\text{ nm}^{-1}$ , corresponding to axial d-spacing characteristic of packing of triacylglycerols, presents in adipose cells (Mykhaylyk et al., 2004).

In order to verify if the differences found for each tissue type, combining WAXS and SAXS techniques, may be useful to characterize them, one parameter of each scattering profiles was extracted. For WAXS, the ratio between the intensity of like-water ( $Q=18.9\text{ nm}^{-1}$ ) and fatty acid ( $Q=13.8\text{ nm}^{-1}$ ) peaks (Griffiths et al., 2007) was used. For SAXS, the intensity of 3<sup>rd</sup> order axial peak (Lewis et al., 2000) was used. These parameters are shown in figure 6 together with their uncertainties. Although few samples were used in this preliminary study, the results combining WAXS and SAXS techniques show that it is statistically possible distinguish among each type of human breast tissue ( $P<0.001$ ).

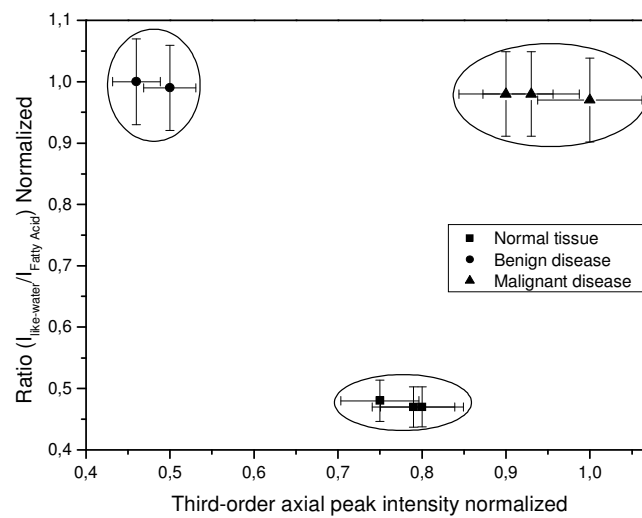


**Figure 6.** Sample distribution on basis of combining of SAXS (third-order axial peak intensity) and WAXS (ratio of like-water and fatty acid peak intensities) parameters, with these uncertainties associated.

#### 4. Conclusion

X-ray scattering experiments applied in human breast tissues, healthy and neoplastic, provide a unique scattering profile to each tissues type, exhibiting features that allows distinguishing among normal, malignant and benign tissues. Using WAXS technique it is possible to find features at molecular level, fatty acid and water, for example, while changes in a supramolecular level, as collagen fibrils, can be observed employing SAXS technique.



Combining both techniques allows correlate changes at molecular and supramolecular levels. Although it is yet beginning, this study shows that the combination of WAXS with SAXS provides a potential medical tool for characterizing small samples of human breast tissues.

## Acknowledges

We would like to acknowledge the support by the Brazilian agency Fundação de Amparo à Pesquisa do Estado de São Paulo (FAPESP) and by the Brazilian Synchrotron Light Laboratory (LNLS) under proposal D11A-SAXS1 4783/05. We also would like to thank the D11A-SAXS1 beam line staff for the help during the experiment.

## References

- Ali, L., Green, E.M., Ellisa, R.E., Bradley, D.A., Grossmannb, J.G., Winlove, C.P., 2004. Study of the molecular and supramolecular organisation of elastic tissue by X-ray diffraction
- Bigi, A. & Roveri, N., 1991. Fibre Diffraction: Collagen Handbook of Synchrotron Radiation, edited by S. Ebashi, M. Koch & E. Rubenstein. (Amsterdan: Elsevier). Vol. 4, 199-239.
- Cunha, D.M., Oliveira, O.R., Perez, C.A., Poletti, M.E., 2006. X-ray scattering profiles of some normal and malignant human breast tissues. *X-ray Spectrom.* 35(6), 370-374.
- Evans, S.H., Bradley, D., Dance, D.R., Baterman, J.E. e Jones, C.H., 1991. Measurements of small-angle photon scattering for some breast tissues and tissue substitute materials. *Phys. Med. Biol.* 36(1), 7-18.
- Falzon ,G., Pearson, S., Murison, R., Hall, C., Siu, K., Evans, A., Rogers, K., Lewis, R., 2006. Wavelet-based feature extraction applied to small-angle x-ray scattering patterns from breast tissue: a tool for differentiating between tissue types. *Phys. Med. Biol.* 51(10), 2465-2477.
- Fernández, M., Keyriläinen, J., Karjalainen-Lindsberg, M.-L., Leidenius, M. von Smitten, K., Fiedler, S., Suortti, P., 2004. Human breast tissue characterization with small-angle x-ray scattering. *Spectroscopy.* 18 (2), 167-176.
- Fernández, M., Keyriläinen, J., Serimaa, R., Torkkeli, M., Karjalainen-Linsberg, M-L., Tenhunen, M., Thomlinson, W., Urban, V., Suortti, P., 2002. Small-angle x-ray scattering studies of human breast tissue samples. *Phys. Med. Biol.* 47(4), 577-592.
- Fernández, M., Keyriläinen, J., Serimaa, R., Torkkeli, M., Karjalainen-Linsberg, M-L., Leidenius, M. von Smitten, K., Tenhunen, M., Fiedler, S., Bravin, A., Weiss, T.M., Suortti, P., 2005. Human breast cancer in vitro: matching histo-pathology with small-angle x-ray scattering and diffraction enhance x-ray imaging. *Phys. Med. Biol.* 50(13), 2991-3006.
- Griffiths, J.A., Royle, G.J., Hanby, A.M., Horrocks, J.A., Bohndiek, S.E., Speller, R.D., 2007. Correlation of energy dispersive diffraction signatures and microCT of small breast tissue samples with pathological analysis. *Phys. Med. Biol.* 52 (20), 6151-6164.
- Hubbell, J.H., Veigele, Wm.J., Briggs, E.A., Brown, R.T., Cromer, D.T., Howerton, R.J., 1975. Atomic form factors, incoherent scattering functions, and photon scattering cross sections. *J. Phys. Chem Ref. Data.* 4 (3), 471-538.
- Kidane, G., Speller, R.D., Royle, G.J., Hanby, A.M., 1999. X-ray scatter signatures for normal and neoplastic breast tissues. *Phys. Med. Biol.* 44 (7), 1791-1802.
- Lewis, R.A., Rogers, K.D., Hall, C.J., Towns-Andrews, E., Slawson, S., Evans, A., Pinder, S.E., Ellis, I.O., Boggis, C.R.M., Hufton, A.P., Dance, D.R., 2000. Breast cancer diagnosis using scattered X-rays. *J. Synchrotron Rad.* 7, 348-352.
- Mykhaylyk, O.O., Smith, K.W., Martin, C.M., Ryan, A.J., 2007. Structural models of metastable phases occurring during the crystallization process of saturated/unsaturated triacylglycerols. *J. Appl. Cryst.* 40: 297-302.
- Oliveira, O.R., Conceição, A.L.C., Cunha, D.M., Poletti, M.E., Pelá, C.A., 2008. Identification of neoplasias of breast tissues using a commercial powder diffractometer. *Journal of Radiation Research* (in press).

- Peplows, D.E., Verghese, K. 1998. Measured molecular coherent scattering form factors of animal tissues, plastics and human breast tissue. *Phys. Med. Biol.* 43(9), 2431-2452.
- Poletti, M.E., Gonçalves, O.D., Mazzaro, I., 2002a. Coherent and incoherent-scattering of 17.44 and 6.93 keV X-ray photons scattered from biological and biological-equivalent samples: characterization of tissues. *X-ray Spectrom.* 31(1), 57-61.
- Poletti, M.E., Gonçalves, O.D., Mazzaro, I., 2002c. X-ray scattering from human breast tissues and breast-equivalent materials. *Phys. Med. Biol.* 47 (1), 47-63.
- Poletti, M.E., Gonçalves, O.D., Schechter, H., Mazzaro, I., 2002b. Precise evaluation of elastic differential scattering cross-sections and their uncertainties in x-ray scattering experiments. *Nucl. Instrum. Methods B.* 187(4), 437-446.
- Pucci-Minafra, I., Luparello, C., Andriolo, M., Basiricò, L., Aquino, A., Minafra, S., 1993. A new form of tumor and fetal collagen that binds laminin. *Biochemistry.* 32, 7421-7427.
- Rogers, K.D., Lewis, R.A., Hall, C., Towbs-Andrews, E., Slawson, S., Evans, A., Pinder, S., Ellis, I., Boggis, C., Hufton, A., 1999. Preliminary observations of breast tumor collagen. *Synchrotron Radiat. News* 12(1): 15-20.
- Round, A.R., Wilkinson, S.J., Hall, C.J., Rogers, K.D., Glatter, O., Wess, T., Ellis, I. O., 2005. A preliminary study of breast cancer diagnosis using laboratory based small angle X-ray scattering. *Phys. Med. Biol.* 50(17), 4159-4168.
- Ryan, E.A., Farquharson, M.J., 2007. Breast tissue classification using x-ray scattering measurements and multivariate data analysis. *Phys. Med. Biol.* 52(22), 6679-6696.
- Speller, R.D., 1999. Tissue analysis using x-ray scattering. *X-Ray Spectrom.* 28(4), 244-250.
- Tartari, A., Casnati, E., Bonifazzi, C., Baraldi, C., 1997. Molecular differential cross sections for x-ray coherent scattering in fat and polymethyl methacrylate. *Phys. Med. and Biol.* 42(12), 2551-2560.
- Tartari, A., Taibi, A., Bonifazzi, C., Gambaccini, M., Felici, M., 2005. Updating of x-ray coherent scattering cross-sections and their effects in microbeam and material analysis applications. *X-ray Spectrom.* 34(5), 421-425.
- Tomal, A., Mazzaro, I., Kakuno, E.M., Poletti, M.E., 2008. Experimental determination of linear attenuation coefficient of normal, benign and malignant breast tissues. Submitted to *Radiat. Phys. Chem.*
- Wilkinson, S. J., Rogers, K. D., Hall, C. J., 2006. Model fitting in two dimensions small angle diffraction patterns from soft tissue. *Phys. Med. Biol.* 51(7): 1819-1830.